Skyrmion lifetime in ultrathin films

Stephan von Malottki,[1,*] Pavel F. Bessarab,[1,2] Soumyajyoti Haldar,[1] Anna Delin,[3,4,5] and Stefan Heinze[1]

[1]*Institute of Theoretical Physics and Astrophysics, University of Kiel, Leibnizstrasse 15, 24098 Kiel, Germany*
[2]*ITMO University, 197101 St. Petersburg, Russia*
[3]*Department of Applied Physics, KTH, Kista, Sweden*
[4]*Department of Physics and Astronomy, Uppsala University, Sweden*
[5]*Swedish e-Science Research Center (SeRC), KTH Royal Institute of Technology, SE-10044 Stockholm, Sweden*

We show that thermal stability of skyrmions due to entropic effects can be strongly affected by external control parameters such as magnetic field and interface composition. The lifetimes of isolated skyrmions in atomic Pd/Fe bilayers on Ir(111) and on Rh(111) are calculated in the framework of harmonic transition state theory based on an atomistic spin model parametrized from density functional theory. Depending on the system the attempt frequency for skyrmion collapse can change by up to nine orders of magnitude with the strength of the applied magnetic field. We demonstrate that this effect is due to a drastic change of entropy with skyrmion radius which opens a route toward stabilizing sub-10-nm skyrmions at room temperature.

Magnetic skyrmions are praised to be information-carrying bits in next-generation data storage and logic devices. The challenge is to obtain long-lived skyrmions at room temperature with a diameter below 10 nm so that emerging technologies based on skyrmions can compete with conventional solutions [1–3]. While room temperature stability has been reported for skyrmions larger than 30 nm in transition-metal multilayers [4,5], sub-10-nm skyrmions have so far been only found in ultrathin film systems at very low temperatures of about 8 K [6–9]. Therefore, an understanding of the mechanisms stabilizing skyrmions and ways to increase their lifetime at ambient temperature are key tasks on the route toward skyrmion-based applications.

The skyrmion lifetime τ as a function of temperature T can conveniently be described in terms of the collapse energy barrier ΔE and the attempt frequency f_0,

$$\tau = f_0^{-1} \exp\left(\frac{\Delta E}{k_B T}\right), \qquad (1)$$

with k_B being the Boltzmann constant. The strong, exponential dependence in Eq. (1) suggests that control over the energy barrier should be the key strategy for improving on thermal stability of skyrmions. Recent theoretical works have indeed focused on obtaining the energy barrier of skyrmion annihiliation [10–20].

For decades, tuning the energy barrier has been the main approach to the development of information storage bits based on magnetic materials. A rule of thumb that the energy barrier should exceed thermal energy by a factor of 40–50 at room temperature to ensure reliable information storage has become an accepted norm (see, e.g., [21,22]). It is important to realize,

however, that such estimates are based on the assumption that the attempt frequency is a constant associated with the Larmor precession, with $f_0 \approx 10^{10}$–10^{12} Hz. Exclusive focus on the energy barrier can lead to biased conclusions about thermal stability when applied to unique objects such as magnetic skyrmions. Some hints for this claim are already present in the literature. Based on Monte Carlo simulations, Hagemeister *et al.* [23] concluded that the attempt frequency for skyrmion nucleation was orders of magnitude larger than that for skyrmion annihilation. Recent theoretical works [10,24] employed statistical approaches to demonstrate that the value of the attempt frequency depends strongly on the mechanism of skyrmion collapse. Experiments by Wild *et al.* [25] showed that small variation of magnetic field leads to a dramatic change in the attempt frequency for annihilation of skyrmions in a B20 compound which was interpreted as an enthalpy-entropy compensation effect.

Here, we demonstrate by means of transition state theory (TST) and *ab initio* electronic structure calculations that sharp sensitivity of the attempt frequency to control parameters such as external magnetic field plays a decisive role in stabilization of nanoscale skyrmions in ultrathin films, exceeding the contribution of the energy barrier. We focus on the collapse of isolated skyrmions in the ferromagnetic background in Pd/Fe atomic bilayers on the (111) surfaces of Ir and Rh. The first system has been extensively studied experimentally [7,8,23,26,27] as well as theoretically [10,11,28–31], while in the latter skyrmions have been recently predicted [32]. We find a pronounced response of the attempt frequency to the applied magnetic field close to the asymptotic divergence of the skyrmion size. We explain this behavior in terms of entropy associated with localized skyrmion eigenmodes which can be strongly affected by the crystal configuration and external magnetic field. The entropy term rises linearly with the skyrmion surface area leading to large lifetime variations for

*Corresponding author: malottki@physik.uni-kiel.de

skyrmions with diameters between 2 and 10 nm. We conclude that exploitation of entropic effects provides an efficient way to control the stability of nanoscale skyrmions.

Within the harmonic approximation to TST, the attempt frequency f_0 for isotropic skyrmion collapse is given by [10]

$$f_0 = \frac{2}{V_0} k_B T \sqrt{\sum_j \frac{a_j^2}{\epsilon_{sp,j}} \frac{\prod_i \sqrt{\epsilon_{sk,i}}}{\prod_i' \sqrt{\epsilon_{sp,i}}}}, \qquad (2)$$

where V_0 is the volume of skyrmion translational modes per unit cell, $\epsilon_{sk,i}$ and $\epsilon_{sp,i}$ are the eigenvalues of the Hessian matrix at the skyrmion state and at the transition state defined by the saddle point (SP) on the energy surface, respectively, and a_j are the components of the velocity normal to the dividing surface. The prime indicates that the negative eigenvalue at the SP is excluded from the product. An SP configuration corresponds to a Bloch pointlike defect centered at an interstitial site of the hexagonal lattice. Therefore, there are two SPs per unit cell of the system, which results in the factor of 2 in Eq. (2). The energy surface as a function of the spin configuration is obtained from an atomistic spin model on a hexagonal lattice which contains the exchange interactions, the Dzyaloshinskii-Moriya interaction, as well as the magnetocrystalline anisotropy energy. All interaction parameters were calculated based on *ab initio* density functional theory (DFT) [11,32]. SPs on the energy surface have been obtained using the geodesic nudged elastic band (GNEB) method [33]. Skyrmion translation costs almost no energy, which is reflected by a very small eigenvalue, $\epsilon_{tr} V_0 \ll k_B T$. As a result, the translational modes are treated as Goldstone modes, leading to the linear temperature dependence of the attempt frequency [10,32].

The attempt frequencies were calculated based on Eq. (2) as a function of applied magnetic field for magnetic skyrmions in Pd/Fe bilayers on Ir(111) and Rh(111) as shown in Fig. 1. Due to the linear dependence on temperature it is convenient to plot f_0/T. While the Fe layer is in fcc stacking, we consider both hcp and fcc stacking of the Pd overlayer as observed in experiments [26]. To compare all systems, the zero of the magnetic field is taken to be the critical field B_c defined as the transition field to the ferromagnetic phase at zero temperature (see Supplemental Material, Table S1 [34]).

For fcc Pd stacking, the attempt frequency decreases by roughly one order of magnitude over the considered field range for both systems. Therefore skyrmions are stabilized by the attempt frequency for increasing fields. As a rough approximation one might still be able to use a constant value of f_0 in this case. A qualitatively different behavior is observed for hcp-Pd/Fe/Ir(111), where the attempt frequency increases by more than seven orders of magnitude for a magnetic field change of 1 T. For hcp-Pd/Fe/Rh(111), the effect is also present at small fields but there is only an increase by one order of magnitude. As a result of the much smaller attempt frequency the skyrmion lifetime is drastically enhanced in ultrathin Fe films with an hcp stacking of the Pd overlayer. The dramatic change in the attempt frequency with the applied magnetic field appears to be a rather general feature of skyrmionic systems as it has also been confirmed for the effective, nearest-neighbor exchange approximation (see Supplemental Material [34]).
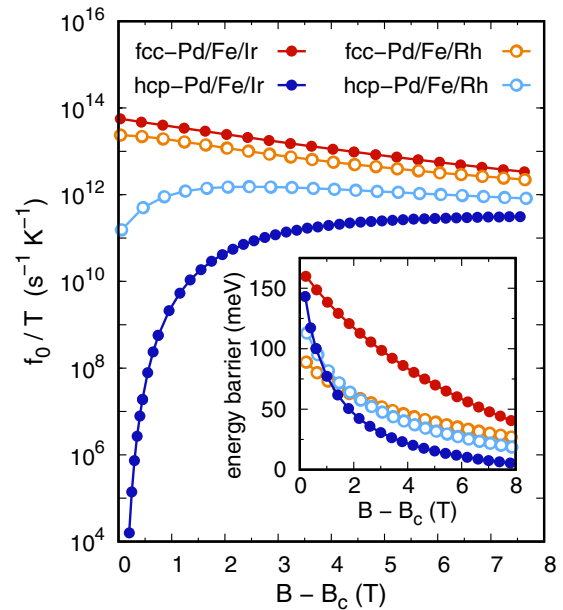

FIG. 1. Calculated attempt frequencies over temperature, f_0/T, for fcc-Pd/Fe and hcp-Pd/Fe bilayers on Ir(111) (filled red and blue circles) and Rh(111) (open orange and light-blue circles) shown on a logarithmic scale over magnetic field strength. The critical field B_c is defined as the transition field to the ferromagnetic phase at zero temperature. f_0 has been calculated with harmonic transition state theory based on DFT parameters for the magnetic interactions. The energy barriers for skyrmion collapse into the ferromagnetic state are presented in the inset.

We combine calculated attempt frequencies with the collapse energy barriers obtained in previous works [11,32] using the GNEB method (see the inset of Fig. 1) in order to access the skyrmion lifetime via Eq. (1). Calculated lifetime of skyrmions in Pd/Fe bilayers on Ir(111) is plotted in Fig. 2 as a function of the applied field and temperature [35]. For both Pd stackings, the largest lifetimes are obtained for small magnetic fields and small temperatures. But while the temperature with a 1 h mean lifetime amounts to $T = 45$ K at the lowest accessible field ($B = 3.2$ T) for the fcc stacking of Pd, this value increases to $T = 75$ K for the hcp stacking at $B = 0.2$ T. On the other hand, at $T = 100$ K the lifetime at these magnetic field values amounts to 40 ns for fcc Pd stacking while it is 10 s for hcp Pd stacking, i.e., nine orders of magnitude larger. Note that the energy barrier is even lower in the case of hcp Pd than for fcc Pd (inset of Fig. 1) and this dramatic effect is solely due to the lower attempt frequency in the hcp case which counteracts the higher energy barrier of the fcc case.

The question arises as to why the attempt frequency displays such a strikingly different behavior for seemingly similar ultrathin film systems. To elucidate the origin of this effect we study the system-dependent terms entering Eq. (2) separately as shown in Fig. 3. The inverse of the Goldstone mode volume V_0 [Fig. 3(a)] is monotonously increasing for all four systems and can therefore not be responsible for the different trends. Additionally, the largest increase by a factor of about 2 takes place in hcp-Pd/Fe/Ir(111) and is much smaller than the discussed effect. The dynamical factor
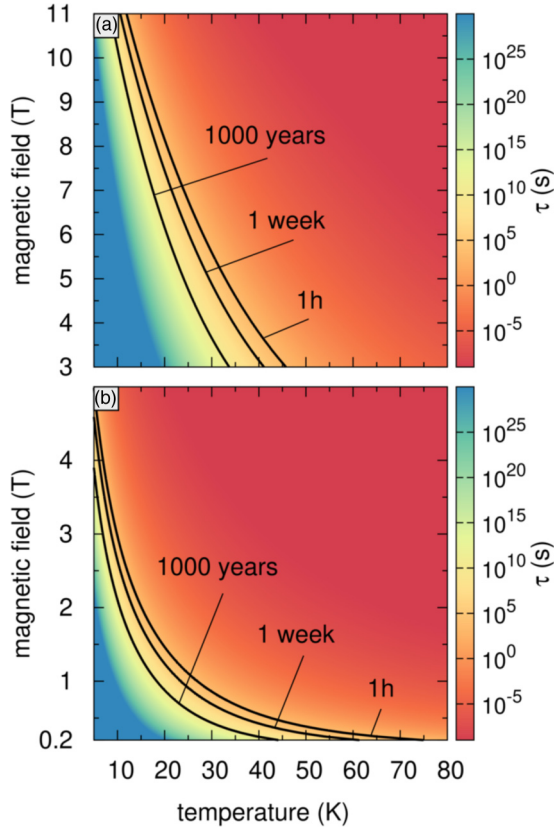
FIG. 2. Mean skyrmion lifetimes for (a) fcc-Pd/Fe/Ir(111) and (b) hcp-Pd/Fe/Ir(111) are displayed by a color map for varying magnetic field strength and temperature. It is calculated by Eq. (1), using data points every 0.05 T and interpolations between these points. For illustration, isolines are given for certain values of mean skyrmion lifetime.

$\tilde{v} \equiv \sqrt{\sum_j a_j^2 / \epsilon_{sp,j}}$ [Fig. 3(b)] increases for Pd/Fe bilayers on Rh(111) and decreases for bilayers on Ir(111). The changes are on an even smaller scale than for the Goldstone mode volumes. Therefore, it cannot be the origin of the trend either.

The third component of Eq. (2) consists of the ratio of the products of the eigenvalues. As shown in the Supplemental Material [34], it describes the contribution of the stable modes to the entropy difference between the transition state and the skyrmion state:

$$\sqrt{2\pi k_B T} \frac{\prod_i \sqrt{\epsilon_{sk,i}}}{\prod_i' \sqrt{\epsilon_{sp,i}}} = \exp\left(\frac{\Delta S'}{k_B}\right). \tag{3}$$

This contribution to the entropy difference is shown on a logarithmic scale in Fig. 3(c). It follows the trend of the attempt frequency and is quantitatively very similar, e.g., it exhibits a decrease in fcc-Pd/Fe/Ir(111) by a factor of ≈ 1.5 and an increase in hcp-Pd/Fe/Ir(111) by about seven orders of magnitude. Clearly, it is the entropy term that defines the response of the attempt frequency to the magnetic field.

The direct comparison of $\Delta S'$ and the skyrmion radius, r [Figs. 3(c) and 3(d)], reveals a correlation between both quantities. Note that the size of the SP excitations are fairly constant with respect to the magnetic field (see Supplemental Material, Fig. S1 [34]) and therefore cannot affect the trend of
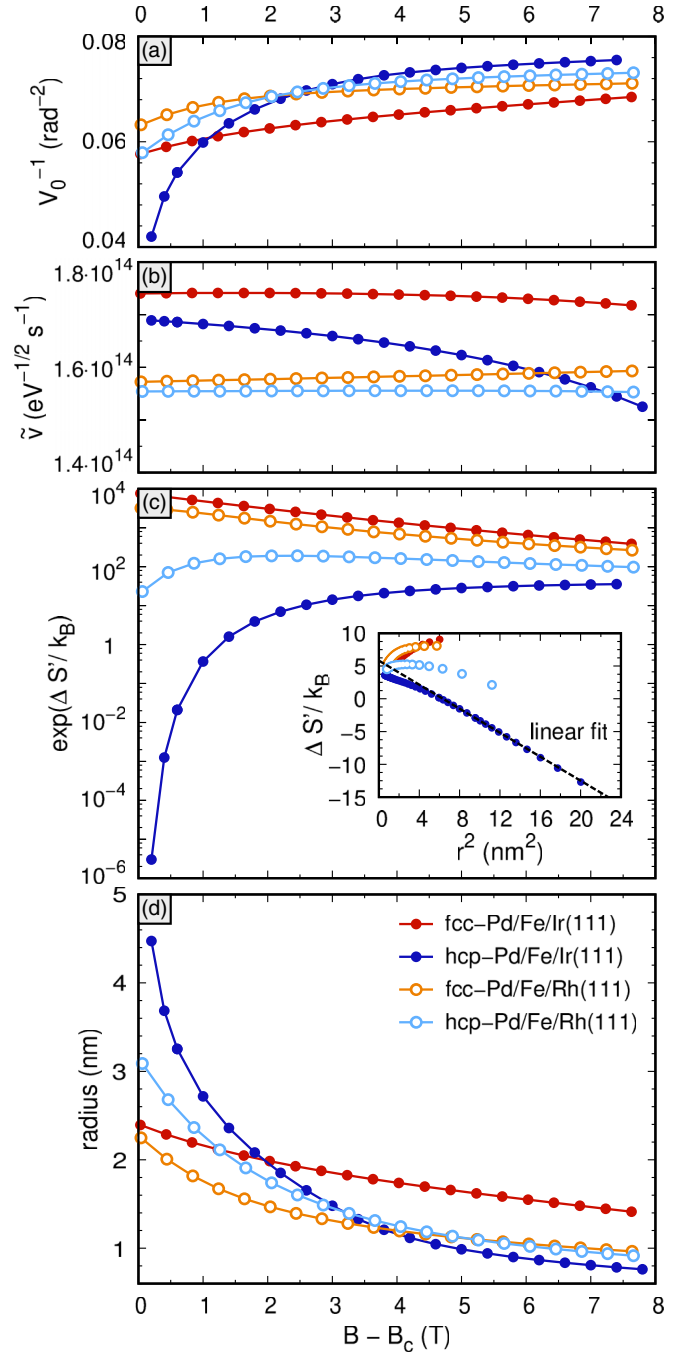

FIG. 3. Terms entering the attempt frequency f_0 as given by Eq. (2) are shown separately as a function of magnetic field strength for Pd/Fe bilayers on Ir(111) and on Rh(111). The inverse of the Goldstone mode volume (a), the dynamical factor $\tilde{v}$ (b), and the entropic factor $\exp(\Delta S'/k_B)$ (c) computed at $T = 100$ K. In the inset of (c) $\Delta S'$ is shown over r^2 and a linear fit has been performed for hcp-Pd/Fe/Ir(111) between 12 and 24 nm². The radius is shown in (d).

the entropy difference. By plotting $\frac{\Delta S'}{k_B}$ vs r^2 [inset of Fig. 3(c)] one can see that the entropy difference associated with the stable modes of hcp-Pd/Fe/Ir(111) decreases linearly with the surface area of the skyrmion for values above $r^2 \approx 4$ nm². This corresponds to magnetic fields below ≈ 2.5 T for which
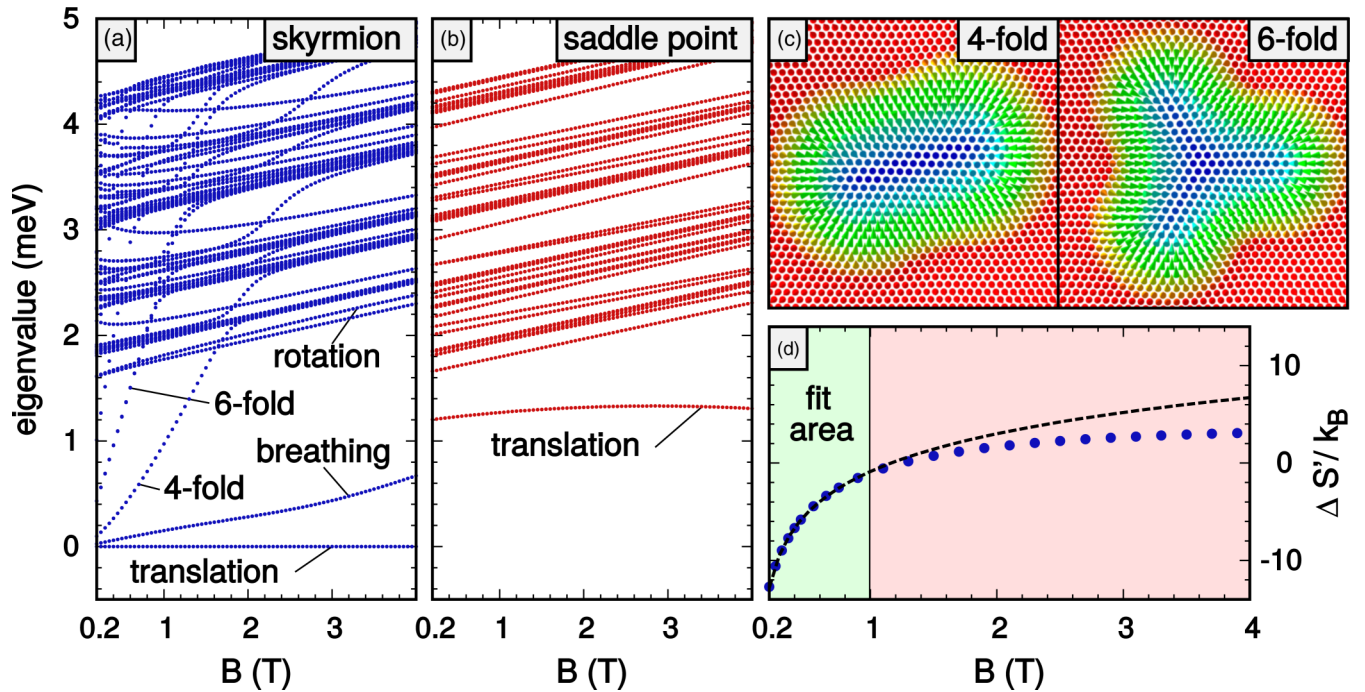
FIG. 4. The calculated eigenvalues of the Hessian matrix are shown for (a) the skyrmion and (b) the saddle point of hcp-Pd/Fe/Ir(111) with varying magnetic field strengths. For the sake of clearness we only show the first 100 out of 9800 eigenvalues for both states. In (c) two skyrmion eigenvalues labeled in (a) are visualized by exciting the skyrmion along the corresponding eigenmodes. In (d) $\frac{\Delta S'}{k_B}$ is fitted by Eq. (4) in the green fit area from 0.2 to 1.0 T.

the radius shows its asymptotic divergence with the applied field. For large fields, far away from the asymptotic behavior, the radius starts to converge to the minimal radius and the entropy difference stops following the surface area linearly. Based on this observation, the magnetic field dependence of the entropy difference and by this of the attempt frequency can be separated into an asymptotic region and a convergence region. This is consistent with both fcc systems whose radii are not asymptotic and their entropy change is not linear in r^2. On the other hand, the radii of hcp-Pd/Fe/Rh(111) suggest the beginning of an asymptotic phase in which its entropy difference starts to follow the surface area linearly. Due to the scaling with skyrmion size we speculate that the entropy effect is even more dramatic for skyrmions in three-dimensional systems, which is consistent with the measurements by Wild *et al.* [25].

To investigate the dependencies of the entropy in more detail, we present the first 100 eigenvalues in Fig. 4 for the skyrmion (SK) and the SP over magnetic field. Most of them are slightly increasing linearly and correspond to magnon or mixed modes in which the magnon modes are excited together with the SK and SP states, respectively. In Eq. (3) most of these contributions should cancel out since they are similar for both states. However, some SK eigenvalues in Fig. 4(a) are increasing with a significantly higher slope in the asymptotic region, crossing the bands of magnon and mixed modes. These eigenvalues belong to pure skyrmion deformation modes whose merge into the magnon continuum is in agreement with an earlier theoretical work on skyrmions in a square lattice [36]. Since these skyrmion modes are only showing this behavior in the asymptotic region, their eigen-

values seem to depend on the skyrmion size. Consistently, the SP eigenvalues do not show this feature since the SP size is not changing with magnetic field (see Supplemental Material, Fig. S1 [34]).

The assumption that only the deformation modes and the breathing mode are contributing to Eq. (3) yields a direct relation of the entropy difference, $\Delta S'$, to the magnetic field:

$$\frac{\Delta S'}{k_B} = A + \frac{n}{2} \ln(B). \qquad (4)$$

The parameter A is the sum of all particular slopes of the skyrmion eigenvalues and n is the number of deformation and breathing modes. By fitting Eq. (4) to the entropy difference over magnetic field [Fig. 4(d)], we found a very good agreement in the asymptotic region. As expected, deviations occur in the convergence region. We obtain $n \approx 10.3$ which is in reasonable agreement with the value of 13 contributing skyrmion modes counted at $B = 0.2$ T from Fig. 4(a). This gives evidence that the pronounced response of the entropy and the attempt frequency on the applied magnetic field are predominantly defined by only a few skyrmion eigenmodes, even though several thousand eigenvalues are entering Eq. (2).

In conclusion, we have demonstrated that a criterion of stability based only on the energy barrier does not hold for magnetic skyrmions at transition-metal interfaces. Due to entropy, the attempt frequency—normally assumed to be constant—can change by orders of magnitude with skyrmion diameter and system and can become the decisive factor for skyrmion lifetime. Our work opens other paths toward stabilizing sub-10-nm skyrmions at room temperature.

---

[1] A. Fert, N. Reyren, and V. Cros, Nat. Rev. Mater. **2**, 17031 (2017).

[2] A. Fert, V. Cros, and J. Sampaio, Nat. Nanotechnol. **8**, 152 (2013).

[3] X. Zhang, M. Ezawa, and Y. Zhou, Sci. Rep. **5**, 9400 (2015).

[4] C. Moreau-Luchaire, C. Moutafis, N. Reyren, J. Sampaio, C. Vaz, N. Van Horne, K. Bouzehouane, K. Garcia, C. Deranlot, P. Warnicke *et al.*, Nat. Nanotechnol. **11**, 444 (2016).

[5] A. Soumyanarayanan, M. Raju, A. G. Oyarce, A. K. Tan, M.-Y. Im, A. P. Petrović, P. Ho, K. Khoo, M. Tran, C. Gan *et al.*, Nat. Mater. **16**, 898 (2017).

[6] S. Heinze, K. Von Bergmann, M. Menzel, J. Brede, A. Kubetzka, R. Wiesendanger, G. Bihlmayer, and S. Blügel, Nat. Phys. **7**, 713 (2011).

[7] N. Romming, C. Hanneken, M. Menzel, J. E. Bickel, B. Wolter, K. von Bergmann, A. Kubetzka, and R. Wiesendanger, Science **341**, 636 (2013).

[8] N. Romming, A. Kubetzka, C. Hanneken, K. von Bergmann, and R. Wiesendanger, Phys. Rev. Lett. **114**, 177203 (2015).

[9] P.-J. Hsu, A. Kubetzka, A. Finco, N. Romming, K. von Bergmann, and R. Wiesendanger, Nat. Nanotechnol. **12**, 123 (2017).

[10] P. F. Bessarab, G. P. Müller, I. S. Lobanov, F. N. Rybakov, N. S. Kiselev, H. Jónsson, V. M. Uzdin, S. Blügel, L. Bergqvist, and A. Delin, Sci. Rep. **8**, 3433 (2018).

[11] S. von Malottki, B. Dupé, P. F. Bessarab, A. Delin, and S. Heinze, Sci. Rep. **7**, 12299 (2017).

[12] I. S. Lobanov, H. Jónsson, and V. M. Uzdin, Phys. Rev. B **94**, 174418 (2016).

[13] V. M. Uzdin, M. N. Potkina, I. S. Lobanov, P. F. Bessarab, and H. Jónsson, Physica B: Condens. Matter **549**, 6 (2018).

[14] S. Rohart, J. Miltat, and A. Thiaville, Phys. Rev. B **93**, 214412 (2016).

[15] P. F. Bessarab, Phys. Rev. B **95**, 136401 (2017).

[16] S. Rohart, J. Miltat, and A. Thiaville, Phys. Rev. B **95**, 136402 (2017).

[17] D. Stosic, J. Mulkers, B. Van Waeyenberge, T. B. Ludermir, and M. V. Milošević, Phys. Rev. B **95**, 214418 (2017).

[18] D. Cortés-Ortuño, W. Wang, M. Beg, R. A. Pepper, M.-A. Bisotti, R. Carey, M. Vousden, T. Kluyver, O. Hovorka, and H. Fangohr, Sci. Rep. **7**, 4060 (2017).

[19] J. Hagemeister, A. Siemens, L. Rózsa, E. Y. Vedmedenko, and R. Wiesendanger, Phys. Rev. B **97**, 174436 (2018).

[20] A. S. Varentsova, M. N. Potkina, S. von Malottki, S. Heinze, and P. F. Bessarab, Nanosyst.: Phys., Chem., Math. **9**, 356 (2018).

[21] F. Büttner, I. Lemesh, and G. S. D. Beach, Sci. Rep. **8**, 4464 (2018).

[22] L. Caretta, M. Mann, F. Büttner, K. Ueda, B. Pfau, C. M. Günther, P. Hessing, A. Churikova, C. Klose, M. Schneider, D. Engel, C. Marcus, D. Bono, K. Bagschik, S. Eisebitt, and G. S. D. Beach, Nat. Nanotechnol. **13**, 1154 (2018).

[23] J. Hagemeister, N. Romming, K. Von Bergmann, E. Vedmedenko, and R. Wiesendanger, Nat. Commun. **6**, 8455 (2015).

[24] L. Desplat, D. Suess, J.-V. Kim, and R. L. Stamps, Phys. Rev. B **98**, 134407 (2018).

[25] J. Wild, T. N. Meier, S. Pöllath, M. Kronseder, A. Bauer, A. Chacon, M. Halder, M. Schowalter, A. Rosenauer, J. Zweck, J. Müller, A. Rosch, C. Pfleiderer, and C. H. Back, Sci. Adv. **3**, e1701704 (2017).

[26] A. Kubetzka, C. Hanneken, R. Wiesendanger, and K. von Bergmann, Phys. Rev. B **95**, 104433 (2017).

[27] C. Hanneken, F. Otte, A. Kubetzka, B. Dupé, N. Romming, K. von Bergmann, R. Wiesendanger, and S. Heinze, Nat. Nanotechnol. **10**, 1039 (2015).

[28] B. Dupé, M. Hoffmann, C. Paillard, and S. Heinze, Nat. Commun. **5**, 4030 (2014).

[29] M. Böttcher, S. Heinze, S. Egorov, J. Sinova, and B. Dupé, New J. Phys. **20**, 103014 (2018).

[30] L. Rózsa, E. Simon, K. Palotás, L. Udvardi, and L. Szunyogh, Phys. Rev. B **93**, 024417 (2016).

[31] L. Rózsa, K. Palotás, A. Deák, E. Simon, R. Yanes, L. Udvardi, L. Szunyogh, and U. Nowak, Phys. Rev. B **95**, 094423 (2017).

[32] S. Haldar, S. von Malottki, S. Meyer, P. F. Bessarab, and S. Heinze, Phys. Rev. B **98**, 060413 (2018).

[33] P. F. Bessarab, V. M. Uzdin, and H. Jónsson, Comput. Phys. Commun. **196**, 335 (2015).

[34] See Supplemental Material at http://link.aps.org/supplemental/10.1103/PhysRevB.99.060409 for information on calculations of the entropy and eigenvalues, skyrmion properties, saddle-point information, and attempt frequency in the effective model.

[35] Similar plots for Pd/Fe/Rh(111) are shown in Ref. [32].

[36] S.-Z. Lin, C. D. Batista, and A. Saxena, Phys. Rev. B **89**, 024415 (2014).